RECENT DEVELOPMENTS IN RADIAL METROLOGY: A COMPUTER-BASED OPTICAL METHOD FOR PROFILING CAVITIES

John A. Gilbert
Department of Mechanical Engineering
University of Alabama in Huntsville
Huntsville, Alabama 35899, USA

Pal Greguss
Applied Biophysics Laboratory
Technical University of Budapest
Budapest, Hungary H-1502

Donald R. Matthys
Physics Department
Marquette University
Milwaukee, Wisconsin 53233, USA

David L. Lehner
Department of Mechanical Engineering
University of Alabama in Huntsville
Huntsville, Alabama 35899, USA

Abstract

Radial metrology is a process devised to study the inner surfaces of cavities found, for example, inside pipes, tubes, and boreholes. This paper describes some recent advances in radial metrology and introduces a new computer-based optical method for profiling cavities. In this method, speckles are projected onto the surface under study and the speckle pattern is digitally recorded and compared to either a reference standard or to other speckle patterns recorded as the cavity changes shape. The apparent speckle movement is computed by numerically correlating small subsets extracted from each pattern. These shifts are used to measure surface deflections or to contour the cavity with respect to a reference shape.

1. Introduction

Recently, a new technique called radial metrology was introduced to make measurements within cavities[1,2]. The measurement system included a panoramic doughnut lens (PDL) which produces a 2-D representation of a 3-D cylindrical surface using Flat Cylindrical Perspective (FCP). The optical transformation performed by the PDL results in an annular FCP image where the width of the image corresponds to the angular field of view measured with respect to the optical axis, and each concentric ring in the image plane is the loci of points recorded at a constant field angle[3].

Figure 1 illustrates one of the optical configurations evaluated for radial metrology. In this example, a device called a radial profilometer is shown inserted into a cylindrical cavity. A diverging laser beam (shown launched from a fiber optic labeled (1)) is directed through a projection lens (2). The beam passes through a panoramic doughnut lens (3) and is collimated and shaped by an appropriately masked collimating lens (4) to produce a thin ring. The ring reflects off a conical mirror (5) and passes through a transparent window (6) onto the test surface (7). The image of the illuminated surface is captured through the transparent window (6) by the panoramic doughnut lens (3) and is projected by the projection lens (2) onto a coherent optical fiber bundle (8). The bundle transmits the image from the device to a computer system where changes in the image can be recorded and analyzed using digital acquisition and processing techniques.

Figure 2 demonstrates how a profilometer can be used to visually detect inclusions located on the inner wall of a pipe. In this case, the laser scan which was originally circular traces out shapes in the image plane which are "similar" to those of the inclusions. As demonstrated by Figure 3, computer algorithms can be applied so that portions of this image may be linearized for viewing and measurement purposes. The resolution and contrast of the image are relatively poor, since the photograph was recorded from a television monitor. The lower portion of the trace represents a constant radial distance from the optical axis of the profilometer to the wall of the pipe. The shape and dimensions of the inclusions can be easily observed and measured with respect to this baseline.

The equations required to analyze Figure 2 and the algorithms used to produce Figure 3 are included in Reference 2. Procedures for calibrating the profilometer and for profiling a cavity are also described in that work. The use of a line scan for profiling requires that the profilometer be moved through the cavity to obtain measurements over the original field of view. This procedure limits functional and real-time capabilities. Ideally, the profilometer should remain stationary during the measurement.

This paper demonstrates that the entire region imaged by the PDL can be profiled using a method initially developed for measuring deflections on the outer surfaces of structural components[4,5]. In this method, artifical speckles are projected onto the component using an ordinary 35 mm projector equipped with a clear glass slide splattered with black paint. Speckle patterns are digitally recorded as the surface changes shape, and the apparent in-plane movements of the projected speckles are computed by numerically correlating small subsets extracted from each pattern. These movements are related to the deflection of the surface with respect to a reference shape.

The following section describes the application of this method to radial metrology and gives an overview of the expressions considered when profiling a cavity.

2. Analysis

Figure 4 defines the cartesian (x,y,z) and cylindrical (r,θ,z) coordinate systems used for the analysis. It is assumed that the optical axis of the measurement system lies along the z-direction. Projected speckles fall on point P at an angle α, and the image of the illuminated surface is captured at an angle β, measured with respect to a radial line lying in the r-z plane. When the surface moves normal to the optical axis, the projected image appears to shift along the z-direction through a displacement w. The corresponding radial displacement r is given by

$$r = \frac{w}{\tan[90 - \alpha] + \tan\beta} \qquad (1)$$

The relationship between r and w is nonlinear, since α and β vary from point to point.

The displacement along the z-direction is mapped into the image plane by the panoramic doughnut lens via a mapping function, f, as follows

$$r' = f[w]. \qquad (2)$$

This function takes into account the magnification factor, and includes the FCP stretching methods used to create a 2-D representation of the 3-D cylindrical surface. Equations (1) and (2) can be combined and

$$r' = g[r]. \qquad (3)$$

The function g[r] is determined by calibrating the measurement system. By measuring r' and knowing g[r], Equation (3) can be solved for r. Once r is established for a known value of θ, the z-coordinate of the illuminated point can be calculated using

$$z = \frac{r}{\sin\alpha}. \qquad (4)$$

The profile of the entire surface in view may be obtained by repeating this procedure for other points in the image as required.

3. Experimental

An experiment was conducted to illustrate a calibration procedure and to demonstrate the method described above. Two 38 mm diameter PDLs, spaced at a distance of 61.7 mm (2.43") apart, were positioned with their optical axes aligned with the Z axis of the coordinate system shown in Figure 4. A circular pipe with an inner radius, R, equal to 52.5 mm (2.07"), was mounted on a kinematic stage and positioned midway between the PDLs with its longitudinal axis also along Z. A speckled slide was projected onto the inner wall of a 43.0 mm (1.69") long section of the pipe using a 35 mm projector and one of the PDLs. A 35 mm camera and the second PDL were used to photograph the speckle pattern with the pipe in its initial position. Four additional photographs were taken as the pipe was translated along the X axis, through four 2.54 mm (0.1") increments. The five photographs were subsequently digitized using a CID camera and stored as digital arrays of 256 x 256 pixels with each pixel assigned a grey level ranging from 0 to 255.

Figure 5 shows a photograph of the the FCP image of the speckle pattern recorded through the PDL with the pipe in its original position. The photograph was digitized so that the center of the annulus, C, was located in the center of the CID array at pixel coordinates C(128,128). Two 15 x 15 pixel subsets were extracted from the pattern with their centers located at points A(222,128) and B(34,128). These diametrically opposed points lie on a line parallel to the direction of translation and are located, midway between the outer and inner edges of the FCP image, 94 pixels away from point C. Ordinary correlation techniques (with Lagrangian weighting for interpixel interpolation) were applied to determine the displacement of the subsets, measured in terms of pixel shift, for each of the four translations. The location of the displaced subset coincides with the point at which the correlation coefficient attains its maximum value.

Table 1 shows the results obtained from the analysis. The pixel shift is measured in the image plane along a radial axis, r', originating from point C; a peak correlation value of 1.0 represents a perfect match.

Table 1

PT.	TRANS. ALONG r	r	PIXEL SHIFT	r'	PEAK CORRELATION
A	-10.16 mm (-0.4")	42.34 mm (1.67")	-15.35	78.65 pixels	.541
A	-7.62 mm (-0.3")	44.88 mm (1.77")	-11.05	82.95 pixels	.735
A	-5.08 mm (-0.2")	47.42 mm (1.87")	-7.05	86.95 pixels	.882
A	-2.54 mm (-0.1")	49.96 mm (1.97")	-3.20	90.80 pixels	.954
A,B	0.00 mm (0.0")	52.50 mm (2.07")	0.00	94.00 pixels	1.000
B	2.54 mm (0.1")	55.04 mm (2.17")	3.00	97.00 pixels	.954
B	5.08 mm (0.2")	57.58 mm (2.27")	6.75	100.75 pixels	.874
B	7.62 mm (0.3")	60.12 mm (2.37")	9.85	103.85 pixels	.776
B	10.16 mm (0.4")	62.66 mm (2.47")	13.20	107.20 pixels	.715

The calibration curve in Figure 6 was established by plotting r versus r', and defines g[r] in Equation (3). Measurements are independent of the z-coordinate, since the optical axis of the measurement system remains parallel to the longitudinal axis of the pipe and the cross section of the pipe is constant. The calibration is valid over a 20.32 mm (0.80") range where the value of r lies between 42.34 mm (1.67") and 62.66 mm (2.47"). In this range, the response is nearly linear with one pixel representing a radial displacement of approximately 0.71 mm (0.028"). A precise value for r may be obtained by selecting a subset centered at a point on the image plane with a given r', and numerically correlating the subset with subsets in the displaced image to compute the pixel shift. The value of r is determined by locating the point corresponding to the selected value of r' on the curve in Figure 7, and then moving up or down the curve through a vertical distance equal to the pixel shift.

4. Discussion

Table 1 shows that the magnitude of the peak correlation decreases with increasing displacement. This can be attributed to the apparent change in the size of the speckles as they move in the FCP image. Speckles moving toward the center of the image are compressed while speckles moving away from the center are elongated. This places a restriction on the range over which displacements can be measured, since peak correlations of less than 0.7 are generally suspect. Future research will focus on the development of computer algorithms to remove this distortion.

The measurement system used to demonstrate the method has some major drawbacks which limit its potential for practical application. A practical device should be packaged so that it can be easily manipulated throughout a cavity to access and profile regions of interest. Future plans include modifying the profilometer shown in Figure 1 to include a means for speckle projection. The advantages of such a device will be that is simple and relatively inexpensive, it can be miniaturized, there will be no moving parts, the image will be continuously displayed in the image plane, and measurements will be completely automated.

Finally, the method of calibration described above has the disadvantage that several speckle patterns must be recorded and analyzed. An alternative method of calibrating the system involves recording only two patterns; the speckle pattern with the pipe in its initial location, and the speckle pattern with the pipe translated along the x-direction through a displacement, u. This procedure will be demonstrated in future work. .

After developing these tools, the authors expect to produce a three-dimensional, full-field computer vision system which will automatically draw an isometric view of a relatively large cavity by recognizing and combining various features of several images taken through the measurement system.

5. Conclusions

This paper discusses some recent advances in radial metrology and describes a profiling method in which measurements are made by digitally recording and numerically correlating artificial speckle patterns projected onto the walls of a cavity. The main advantages of this method are that it can be applied to any surface, it is non-contact and non-destructive, and the analysis can be completely automated. The method offers the potential to vary measurement sensitivity over a wide range and to access occluded or remote areas by using fiber optic components.

Future plans for improving the method were also discussed. These included the plans for the design and construction of a practical measurement device, the development of computer algorithms to correct for speckle distortion in the acquired images, and refinements in the method used for calibrating the measurement system.

6. Acknowledgements

The authors wish to thank J.L. Lindner of UAH for helping with the experiments. Research in the area of profiling is being funded under contract by the Alabama Research Institute. MSFC/NASA supports work in radial metrology under Grant No. NAS8-686.

7. References

1. Gilbert, J.A., Greguss, P., Lehner, D.L., Lindner, J.L., "Radial profilometry," Proc. of the 1987 Joint SEM-BSSM International Conference on Advanced Measurement Techniques, London, England, August 24-27 (1987).

2. Greguss, P., Gilbert, J.A., Matthys, D.R., Lehner, D.L., "Developments

in radial metrology," Proc. of SPIE International Symposium on Optical Engineering and Industrial Sensing for Advanced Manufacturing Technologies, Dearborn, Michigan, June 25-30 (1988).

3. Greguss, P., "The tube peeper: a new concept in endoscopy," Optics and Laser Technology 17, 41-45 (1985).

4. Gilbert, J.A., Matthys, D.R., Taher, M.A., Petersen, M.E., "Shadow speckle metrology," Applied Optics 25(2), 189-203 (1986).

5. Gilbert, J.A., Matthys, D.R., Taher, M.A., Petersen, M.E., "Profiling structural members using shadow speckle metrology," Optics and Lasers in Engineering 8(1), 17-27 (1988).

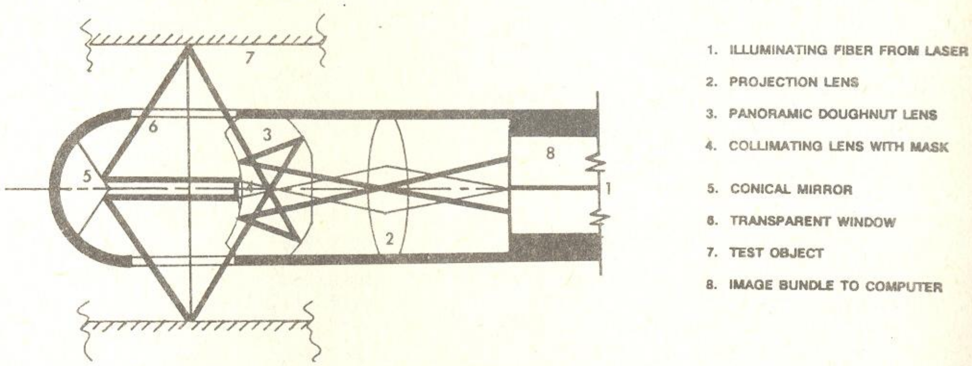

Fig. 1. Schematic diagram of a radial profilometer.

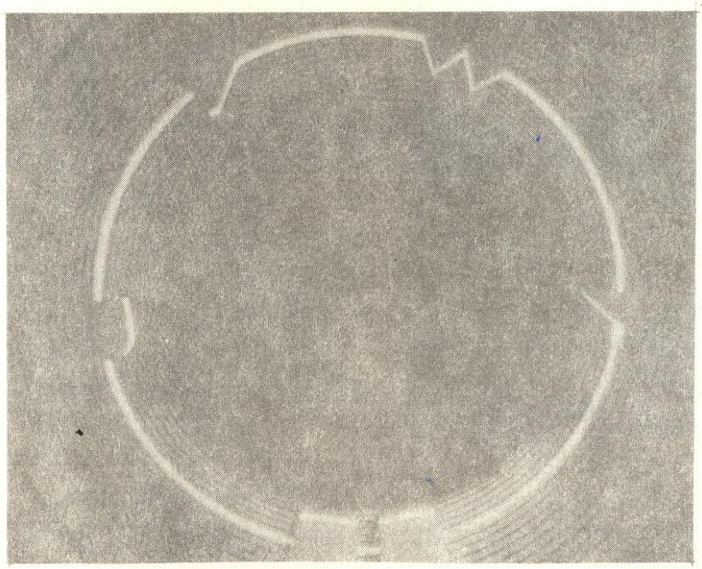

Fig. 2. FCP image taken through a PDL showing the trace obtained when inclusions are placed on the inner wall of a cylindrical pipe.

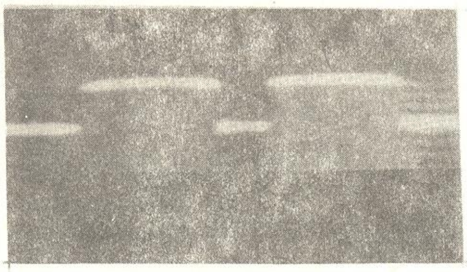

Fig. 3. Digitized image after applying a transformation algorithm to a portion of the image shown in Fig. 2.

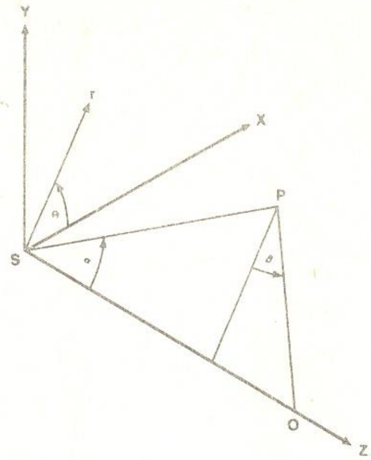

Fig 4. Coordinate axis system used for analysis.

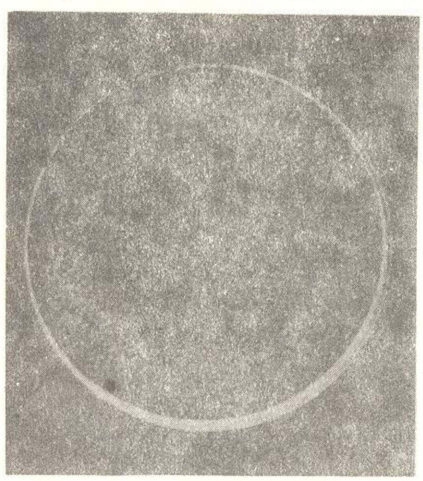

Fig. 5. Image of the projected speckle pattern with the pipe located symmetrically with respect to the optical axis of the measurement system.

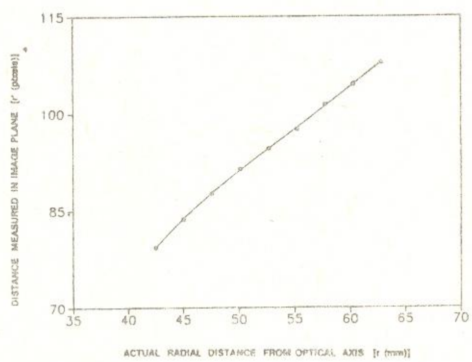

Fig. 6. Calibration curve for displacements ranging over 20.32 mm (0.8").